FINAL REPORT

for

NGR 21-002-390

Entitled

RESEARCH CONCERNING THE GEOPHYSICAL CAUSES AND MEASUREMENT ACCURACIES RELATED TO THE IRREGULARITIES IN THE ROTATION OF THE EARTH

Period Covered: December 11, 1972 - October 10, 1975

by

Douglas G. Currie
Principal Investigator

(NASA-CR-155732) RESEARCH CONCERNING THE GEOPHYSICAL CAUSES AND MEASUREMENT ACCURACIES RELATED TO THE IRREGULARITIES IN THE ROTATION OF THE EARTH Final Report, 11 Dec. 1972 - 10 Oct. 1975 (Maryland Univ.) HC A04/MF A01
N78-17527
Unclas
G3/46 04503

Submitted to

GODDARD SPACE FLIGHT CENTER
NATIONAL AERONAUTICS AND SPACE ADMINISTRATION

February 1978

UNIVERSITY OF MARYLAND
DEPARTMENT OF PHYSICS AND ASTRONOMY
COLLEGE PARK, MARYLAND

ABSTRACT

The primary objective of this effort consisted of a detailed study of the history of the motion of the moon. More precisely this grant has resulted in the support of David Rubincam in the preparation of "The Early History of the Lunar Inclination". This has consisted of the completion of his thesis within a cooperative program between the University of Maryland and the Goddard Space Flight Center. In addition, several analyses were developed which are related to the determination of the effect of various refractive phenomena on the accuracy of measurements made through the earth's atmosphere.

TABLE OF CONTENTS

I. GENERAL DISCUSSION

The primary effort supported by this grant consisted of a research study, conducted by David Rubincam, entitled "The Early History of the Lunar Inclination". This study and the resultant thesis was in the form of a cooperative program directed by Dr. John O'Keefe of the Goddard Space Flight Center and the Principal Investigator at the University of Maryland. The objective of this study was to evaluate the lunar motion by numerically integrating lunar motion backward in time to an epoch when the moon was much closer to the earth and the inclination of the orbit was much greater than the current value. At this time the value and the role of viscosity of the earth in order to correct errors which had been made by investigators using earlier analyses. These errors had lead to improper conclusions on the mode of formation of the earth-moon system.

The full description of this work and a discussion of the results is contained in the thesis presented to the University of Maryland by Mr. Rubincam. In addition, this material is also presented in a Goddard Space Flight Center Technical Document #X-592-73-328.

Rather than repeat this discussion or attach the thesis in full to this final report, certain particularly relevant sections are presented in the next section. These include the abstract, the acknowledgments, and the table of contents which indicates the full range of topics addressed within the thesis. The introduction illustrates the basic method of attack. The discussion section contains the technical conclusions from the mathematical treatment and the implications on the formation of the earth-moon system.

II. THE EARLY HISTORY OF THE LUNAR INCLINATION

THE EARLY HISTORY
OF THE LUNAR INCLINATION

David Parry Rubincam

ABSTRACT

The effect of tidal friction on the inclination of the lunar orbit to the earth's equator for earth-moon distances of less than 10 earth radii is examined. The results obtained bear on a conclusion drawn by Gerstenkorn and others which has been raised as a fatal objection to the fission hypothesis of lunar origin, namely, that the present nonzero inclination of the moon's orbit to the ecliptic implies a steep inclination of the moon's orbit to the earth's equatorial plane in the early history of the earth-moon system. This conclusion is shown to be valid only for particular rheological models of the earth. In the case of a viscous earth, the results indicate that the problem of wrenching the moon out of an equatorial orbit into an inclined orbit to account for the present tilt of the lunar orbit to the ecliptic must be faced in the accretion theory of the moon's origin and possibly the capture theory, as well as in the fission theory. In this respect all three theories are on the same footing. A solution to the inclination problem is presented.

The treatment of tidal friction adopted here employs the approach of George Darwin and pursues his suggested solution to the inclination problem in great detail. The earth is assumed to behave like a highly viscous fluid in response to tides raised in it by the moon. The moon is assumed to be tideless and in a circular orbit about the earth. The equations of tidal friction are integrated numerically to give the inclination of the lunar orbit as a function of earth-moon

distance. It is found that if the radius of the lunar orbit is greater than 3.83 earth radii, then the inclination of the moon's orbit to the earth's equator will increase if the moon is perturbed from an equatorial orbit, provided the earth's viscosity is greater than 10^{16} poises. The present inclination of the lunar orbit to the ecliptic can be explained if the moon's orbit is perturbed about 3° out of the equatorial plane at 3.83 earth radii, provided that the earth's viscosity is not less than 10^{18} poises. It is also found that if the viscosity is large (greater than 10^{16} poises), then, under certain conditions, the radius of the moon's orbit may actually decrease temporarily, and then increase; and further, that an upper limit can be placed on the inclination of the lunar orbit to the earth's equator when the moon is 3.83 earth radii distant from the earth, regardless of the moon's prior history.

ACKNOWLEDGMENT

First and foremost, I wish to express my gratitude to Dr. John A. O'Keefe of Goddard Space Flight Center for pointing out to me the problem of the lunar inclination and advising me on it. Working with Dr. O'Keefe has been a most rewarding and pleasurable experience.

Next, my thanks go to Dr. David E. Smith of Goddard Space Flight Center and Dr. Douglas G. Currie of the University of Maryland. Dr. Smith's moral and financial support were invaluable. Dr. Currie's willingness to help me and his shrewd insights are greatly appreciated.

I would also like to express my appreciation to Edward Kelsey, Drs. Michael A'Hearn, Ernst Öpik, and Vincent Minkiewicz, all of the University of Maryland, and Dr. Louis S. Walter of Goddard Space Flight Center for their encouragement, suggestions, and comments.

Computer time and facilities were made available for this study by Goddard Space Flight Center and the University of Maryland Computer Science Center.

TABLE OF CONTENTS

TABLE OF CONTENTS (Continued)

LIST OF TABLES

LIST OF FIGURES

LIST OF FIGURES (Continued)

INTRODUCTION

Men have speculated about the tides for centuries. An ancient Chinese scholar suggested that the earth lived, that the ocean was its blood, and that the tides were the beating of the earth's pulse (Darwin 1962, pg. 76). An Arabian scholar explained the rising of the tide as being caused by the heating of the ocean by sunlight and moonlight (Darwin 1962, pp. 77-79). Others also suggested that the tides were somehow caused by the sun and moon (Darwin 1962, pp. 79-85), but it remained for Isaac Newton to advance the correct explanation for the cause of the tides (Newton 1966). Newton realized that the lunar tides were caused by a combination of gravitational pull and centrifugal effects which would make the water in the oceans collect on the sides of the earth directly under and directly away from the moon, thus giving the earth a bulge. A similar argument holds for the solar tides.

Newton's theory of the tides was carried forward, notably by Bernoulli, Laplace, Darwin, and Kelvin (Darwin 1962, pp. 86-88) to explain the rise and fall of the oceans on the earth. Their efforts culminated in the work of Doodson and Proudman (Doodson 1958).

George Howard Darwin, son of the famous Charles Darwin, considered not only the problem of the tides raised on the earth by the moon, but also a more subtle problem: the action of the tides on the motion of the moon (Darwin 1880). He included in his investigations not only ocean tides, but also tides raised in the bulk of the earth as well; these latter tides are called earth or body tides. Darwin recognized that friction attending the tides, whether they are raised in the oceans or in the earth, would have profound effects on the moon's orbit. In fact, tidal friction dominates the secular change in the moon's orbital elements.

Darwin assumed the earth to be a homogeneous, incompressible viscous fluid in which tides were raised by the moon; the moon itself was assumed to be a point-mass. He expanded the tidal disturbing function in a Fourier series and integrated the equations for the secular change of the moon's orbital elements backwards in time in an attempt to uncover the past history of the moon. Darwin found that the moon orbited very close to the earth at some time in the distant past. He speculated that the earth and moon were once a single primitive body, and that resonance vibrations set up in the body by the sun caused the body to fission, thus throwing the moon into orbit about the earth. Tidal friction then caused the moon to move away from the earth to its present distance.

Jeffreys (1930) found that dissipation in the primitive body would be so great that the vibrations would be damped out, making it impossible for the moon to be torn out by the action of the sun. The fission theory of the origin of the moon fell out of favor. It has been reproposed in more recent times by Cameron (1963), Wise (1963), and O'Keefe (1969).

Modern interest in tidal friction was rekindled by Gerstenkorn (Alfven 1963), who invoked tidal friction in a new hypothesis of lunar origin: capture of the moon. Gerstenkorn's analysis lead him to propose that the moon was once an independent planet in an orbit which carried the moon close to the earth. The tidal interaction between the moon and earth captured the moon in a retrograde orbit, which subsequently flipped over into the prograde orbit we see today. MacDonald (1964) supported a many-moon hypothesis of lunar origin to overcome a time-scale difficulty in tidal evolution. Singer (1968) investigated the problem of prograde capture, while the analysis of Goldreich (1966) lead him to favor accretion of the moon from a swarm of particles in orbit about the earth.

The problems associated with the intimately connected questions of the moon's origin and its orbital evolution are seen to be of surpassing interest today. We will investigate here one of the problems of the early history of the moon: the inclination of the lunar orbit.

CHAPTER V

DISCUSSION

A. Critique of Assumptions Made

We shall now examine the important assumptions made in obtaining our results for strong tidal friction.

One important assumption we have made is that the orbit of the moon remains circular throughout its history, i.e. the eccentricity e of the lunar orbit is zero. The work of Darwin (1880, Section V), Singer (1968), and MacDonald (1964) shows that weak tidal friction decreases the eccentricity as we look back into the past until the moon reaches about 3 earth radii from the earth, where the eccentricity undergoes rapid changes. Since the present value of the eccentricity is 0.055, this would imply that neglect of the eccentricity when the moon was at the reference distance of 3.83 earth radii would lead to negligible error in considering weak tidal friction.

However, use of Darwin's treatment of the eccentricity for viscosities greater than 10^{17} poises indicates that e increases with time until the moon reaches about 16 earth radii distance from the earth; at larger distances the eccentricity rapidly decreases. This indicates that the eccentricity could have been large for earth-moon distances of less than 16 earth radii. However, a nearly circular orbit for the moon over its whole history is by no means excluded. The earth could have behaved as though it had a large viscosity when the moon was less than 16 earth radii from it; beyond 16 earth radii the earth could have behaved as though it had a small viscosity. If this were the case, then if the moon were in a nearly circular orbit at 3.83 earth radii, the eccentricity would slowly grow to its present value as the moon moved outward to its present distance.

Another assumption which we have made is that harmonics higher than the second degree may be neglected in the tidal disturbing function (Equation II-4). To show that this approximation is a good one, we note that the second degree harmonics in the disturbing function are multiplied by $\left(\frac{a}{r}\right)^6$, where a is the radius of the earth and r is the earth-moon distance; this may be seen from Equations (II-3) and (II-4). If third degree harmonics were included in the disturbing function, then they would be multiplied by $\left(\frac{a}{r}\right)^8$; likewise, fourth degree harmonics would be multiplied by $\left(\frac{a}{r}\right)^{10}$, etc. Hence the third degree terms are reduced by a factor of $\left(\frac{a}{r}\right)^2$ from the second degree terms. For $r = 3.83a$, $\left(\frac{a}{r}\right)^2 = 0.068$. Also, the contribution of the third degree tides to the rate of change in time of the inclination is small compared to that of the second degree tides (see the discussion in the last paragraph of this section). Thus the restriction to the second degree terms in the disturbing function leads to only a small error.

We have further assumed that the moment of inertia of the earth C had its present-day value of 8.11×10^{40} g-cm^2 = 0.33 Ma^2. This implies that the earth's core had already formed. Darwin assumed that the earth was homogeneous ($C = 0.4$ Ma^2), as well as incompressible, etc., for reasons of tractability in solving for the response of the earth to the tidal force. Changing the moment of inertia to its value for a homogeneous earth would lead to only slight corrections in our results.

Heating of the earth by the dissipation associated with the friction does not appear to be significant. The energy deposited in the earth as the moon moves from the Roche limit at 2.89 earth radii to 3.83 earth radii amounts to 1.43 ×

10^{36} ergs. Assuming a specific heat of 10^7 ergs/g-deg, the average change in temperature of each gram of matter in the earth is only 24°K.

Our most crucial assumption was that the earth behaved like a highly viscous liquid ($\nu >> 10^{15}$ poises). Whether the earth could have behaved in this manner when the moon was at 3.83 earth radii depended upon the rheological properties of the earth at that time; these properties are unknown.

O'Keefe (1972) points out that since the tidal potential varies like the inverse cube of distance (Equation A-6, Appendix A), the tidal forces acting on the earth were 4000 times greater when the moon was at 3.83 earth radii than they are today, so that the material in the earth may have been near the elastic limit. In such circumstances the earth may have behaved like a highly viscous liquid.

At the present time the mantle of the earth responds to the tidal forces like an anelastic solid, with the tidal lag angles being small (MacDonald 1964). However, the mantle responds to deformations of the earth's surface caused by ice loads as though it had a viscosity of about 10^{21} poises (Gutenberg 1959, Chapter 9), requiring thousands of years to rebound after the removal of the loads. (This may be explainable in terms of diffusion creep; see Kaula 1968, pgs. 101-104). Now the period of the O tide with speed $n - 2\Omega$ is given by $2\pi/(n - 2\Omega)$, so that the period ranges from infinity to about 5 hours as the moon moves through 3.83 earth radii distance. Hence if the earth has a characteristic response time between these two extremes, then it should be excited by the O tidal force as the moon passes through 3.83 earth radii. If the dissipation were great, then the lag angle of the tide would be large. Hence it is by no means clear that the earth would not respond as we have assumed, even with the present internal conditions in the earth, where the characteristic response time is thousands of years.

Our last important assumption was that the moon may have been perturbed out of an equatorial orbit by 2.5 to 3° at 3.83 earth radii distance from the earth, thus explaining the present inclination of the lunar orbit to the ecliptic. Whether the moon could suffer such a perturbation is not clear; conditions at that time may have been chaotic enough to produce it. However, several sources of the perturbation may be ruled out. The first obvious source of perturbation is a collision of a large meteoritic object with the moon. If such a collision occurred, then large amounts of meteoritic nickel might be expected to spatter over the moon's surface*. Large amounts of nickel are not observed in lunar samples. The third degree harmonic in the earth's figure will not give rise to long period perturbations in the inclination if the moon's orbit is circular. Further, it may be shown from Equation 38 of Kaula (1964) that the tides associated with the third degree harmonics in the tidal disturbing function give $\frac{d\psi}{dt} \propto \psi$, just as in the second degree harmonics, but that these terms are much less important than those discussed here. Also, the disturbance in the inclination caused by the precession of the earth's axis and the moon's orbit may be shown to be quite small ($\ll 1°$). The question of the source of the perturbation remains open.

B. Relation of the Results to Theories of the Moon's Origin

We will now examine how our results relate to the theories of the origin of the moon. The three principal theories, namely fission, accretion, and capture are reviewed by Kaula (1971).

Darwin (1880) proposed that a primitive body rotating with a period close to its natural oscillation period was disrupted into the earth and moon by resonance oscillations induced in it by the sun. (That this was not at all likely was shown

*I am indebted to Dr. O'Keefe on this point.

by Jeffreys 1930.) The moon would necessarily be thrown out in the equatorial plane of the earth. Darwin was forced to assume that the primitive earth had a very high viscosity to solve the inclination problem. He derived Equations (III-21) and (III-22) which give rate of change of inclination with distance in the limit of infinite viscosity. After commenting on the absurdity implied by the equations that the rate of change of angle was infinite when the earth rotated twice as fast as the moon revolved, he assumed that the viscosity merely had to be very large to increase the inclination of the moon's orbit to the equatorial plane from an infinitesimal disturbance to an appreciable angle. Darwin took this as the solution to the inclination problem and let the matter rest.

Our detailed analysis (Chapter III) shows that the initial perturbation in the inclination of the moon's orbit to the earth's equator must be about 2.5-3.0° to explain the present inclination, with the viscosity of the earth being greater than 10^{17} poises.

O'Keefe (1969) in his version of the fission theory suggested that the primitive body had greater mass and twice the angular momentum of the present earth-moon system. As the primitive body spun up, its figure progressed along the sequence of the well-known Jacobi ellipsoids and pear-shaped figures (Jeans 1961) until it fissioned into the earth and moon. The system then lost mass and angular momentum through intense heating. While taking over Darwin's results, O'Keefe further suggested that even if the earth were molten after the moon and earth separated, the moon's orbital evolution would not begin until the earth cooled off appreciably, so that the moon would not arrive at 3.83 earth radii until the earth's viscosity was quite high.

In Chapter III, Section D, we investigated the orbital evolution of the moon as the earth cooled off for a number of different activation energies and coefficients in Equation (III-23). In view of the wide variety of results obtained in the temperature of the earth when the moon arrives at 3.83 earth radii, it appears that the self-regulating mechanism proposed by O'Keefe does not exist.

The accretion theory states that the moon formed from a ring of particles in orbit about the earth. The particles collided with each other and stuck together, ultimately building up into the moon.

The ring of particles would be expected to lie in the proper plane. The orbits of particles inclined to the proper plane would precess, thus lowering the chances of collision; at least all the orbits would intersect the proper plane, favoring accretion there. If the moon accreted from the ring much beyond 3.83 earth radii, then the moon would tend to remain near the proper plane, so that its present inclination to the ecliptic could not be explained. However, if the moon formed in ~~the~~ proper plane within 3.83 earth radii (essentially in the equatorial plane), then the mechanism proposed here for driving the moon out of the earth's equatorial plane could have come into play.

At any rate, regardless of how the moon arrived at 3.83 earth radii in the equatorial plane of the earth, whether by fission or accretion, if the viscosity of the earth was greater than 10^{17} poises, and the moon suffered a 2.5-3.0° perturbation in inclination at 3.83 earth radii, then the present inclination to the ecliptic could be explained.

The capture theory has a simple answer to the inclination problem: the moon was captured in a highly inclined orbit to begin with and tidal friction has acted to decrease the inclination to its present value (Gerstenkorn 1969, MacDonald 1964). Of course, these theories begin with the present inclination of the moon's orbit to the ecliptic and solve the equations of tidal friction backward in time to discover the moon's inclination at capture.

These theories once again assume weak tidal friction with small lag angles. However, if the viscosity of the earth is greater than 10^{16} poises, and the moon arrives at a distance less than 3.83 earth radii in an inclined orbit, then the inclination must drop below the critical angle ψ_c before the orbit can expand past 3.83 earth radii (Chapter III, Section B). Thus for large viscosities (greater than 10^{17} poises) the orbit becomes nearly equatorial and we are faced with the same problem as before.

C. Summary of the Important Results

Assuming that the earth behaves like a viscous liquid in responding to the tidal force, and that the moon is in a circular orbit about the earth, with the inclination of the lunar orbit to the earth's equator $\lesssim 20°$, then:*

(a) If the moon is less than 3.83 earth radii distance from the earth and the inclination of the orbit to the earth's equator is steep, then the orbit may contract and then expand, provided the viscosity of the earth is greater than 10^{17} poises. The orbit will expand monotonically if the viscosity is less than 10^{16} poises regardless of the inclination.

(b) The inclination of the lunar orbit to the earth's equator will decrease or remain zero if the moon is closer to the earth than 3.83 earth radii, regardless of the viscosity.

(c) The inclination of the lunar orbit to the earth's equator must be less than 2.7° when the moon is at 3.83 earth radii if the earth's viscosity is 10^{18} poises; at higher viscosities the inclination must be even lower.

(d) The lunar orbit will expand monotonically if the moon is at a distance greater than 3.83 earth radii from the earth, regardless of the viscosity.

---

*$\lesssim 20°$ so that Equations (III-9) through (III-12) hold.

(e) The inclination of the lunar orbit to the earth's equator will increase, or decrease (or remain zero) for earth-moon distances greater than 3.83 earth radii depending upon whether the viscosity of the earth is greater than, or less than 10^{16} poises.

(f) If the viscosity of the earth is greater than or equal to 10^{18} poises, <u>and</u> the plane of the lunar orbit is perturbed about 2.5 to 3 degrees out of the equatorial plane of the earth when the moon is just beyond 3.83 earth radii, then the present five degree inclination of the moon to the ecliptic may be explained.

III. Comments on Atmospheric Refraction

In order to generally address the questions on the formation of the earth-moon system which were raised in the analysis presented by the previous section, precise measurements of the current motion of the earth-moon system are required. The Principal Investigatory has been involved with several of the current techniques which are either now in use or are candidates for future application (i.e. Laser Ranging to Lunar Corner Reflectors Laser Ranging to Artificial Satellites, classical Astrometric techniques with PZT's and Very Long Baseline Amplitude Interferometry in the optical domain).

All of these techniques are, or will be, limited in their ultimate accuracy by large scale refractive phenomena in the earth's atmosphere. Prior to this grant, a preliminary study was initiated on special techniques to use the optical dispersion of the earth's atmosphere, in conjunction with measurements performed at more than one wavelength, to sense the magnitude of this large scale errors and provide data for their correction.

Under this grant, these general methods were studied in more detail. Certain general problems on calibration of the water vapor content were also addressed.

As an illustration of this type of work two subsequent studies, to which the studied conducted under NGR 21-002-390 contributed and which used the tools developed under this grant, are attached as appendices.

The first appendix contains a theoretical analysis of the techniques of using observations at Two Color Technique for measuring of the atmospheric refraction. This data has the format which may be used to correct a PZT observation for this large scale effort. Appendix I also contains a discussion of a hardware technique to implement this theoretical analysis.

The second appendix discusses the use of the basic Two Color Techniques (by which one may use the measurements at two different wavelengths) in Very Long Baseline Amplitude Interferometry. Here again this data may be used to correct the systematic error introduced by the atmosphere. This section generally reviews the technique. This portion of the work under this grant (NGR 21-002-390), consisted of the exploration of a number of the important specific questions which are raised in this discussion.

In addition, several analyses were conducted concerning empirical techniques to correct for the systematic atmospheric effects which are related to the lunar motion, as they applied to laser ranging application.

APPENDIX I

PRECISION STELLAR CATALOGS AND THE ROLE OF ANOMALOUS REFRACTION

PRECISION STELLAR CATALOGS AND THE ROLE OF ANOMOLOUS REFRACTION

by

Douglas G. Currie

UNIVERSITY OF MARYLAND

DEPARTMENT OF PHYSICS AND ASTRONOMY

COLLEGE PARK, MARYLAND

TABLE OF CONTENTS

I. INTRODUCTION

Atmospheric refraction, with its non-predictable variations, is one of the dominant sources of error in the precise determination of the apparent position of a star. It appears that this will be the dominant error source for the new generation of instrumentation now being installed for the determination of stellar catalog and Universal Time (i.e., the USNO 65-cm PZT). The effects of anomolous refraction measurements of stellar position propogate to the various quantities derived from this data. This includes the compilation of stellar catalogs, the determination of Universal Time, and variations in the latitude.

A unique instrument, the Two-Color Refractometer, can, for the first time, directly measure the total deviation which the light of a star suffers due to refraction and thus can be used in a measurement program to evaluate the various aspects of anomolous refraction. In addition, this system may be used to make fundamental astrometric observations which are free from the deleterious effects of refraction.

A. Atmospheric Refraction

There are two aspects of refraction errors which are useful to discuss separately. The first of these effects are the short-term errors or the "random error" in an individual measurement. These errors affect an individual measurement so that it may be significantly different from measures made before and after it on the same night. This type of error may be of the order of 0.15 arc-seconds or larger. When we later discuss all of the errors more generally in terms of the power spectra of the anomolous zenith refraction, the random error is characterized by the magnitude of the power spectra in the domain having periods of a few minutes.

The many individual measurements may be analyzed and the results averaged together for an entire night. This procedure should result in an improved determination of the quantities derived from the stellar position measurements. The improvement should be parameterized by a factor proportional to $1/\sqrt{n}$. This will occur if the errors of each separate measurement are independent. However, if there are phenomena which affect the anomolous refraction which have long periods, then the determination of the averaged quantities may now show this improvement. Again, discussing the question in terms of the power spectra, one will obtain the improvement in performance only if the power spectra vanishes for periods longer than a few minutes. We now address the effects of the power spectra for periods greater than the time which is required for a single observation. The systematic error to be expected may be derived from the power spectra and it will be dominated by the magnitude of the power spectra with the period in question.

B. Derivation of Star Catalogs

We wish now to consider the question of the improvement of the star catalogs. This will require one to both improve the measurement of the single observation and reduce the systematic errors obtained when averaging data over long periods. The former will improve the basic random error and the latter will insure that the result of many measurements will reduce this diminished random error in proportion to $1/\sqrt{n}$. In general, the stellar catalog measurement using the Transit Circle is most affected by three types of error. These are: the anomolous refraction, the encoder errors, and the lack of stability of the personal equations. It is difficult to separate the effects of these errors prior to the measurements of anomolous refraction. Therefore, we shall address the remaining remarks to measurements made with the Photographic Zenith Tube (PZT). For the PZT, the errors of encoders and lack of reproducibility of personal equation are far less significant than in the Transit Circle. In addition, to first order one is independent of normal refraction and only sensitive to the anomolous refraction. In this discussion, we refer to the "normal refraction" as that theoretical quantity derived from the zenith distance of the star, and the local pressure, temperature, and humidity. The anomolous refraction is the difference between this normal or calculated refraction and the actual measured refraction.

In the case of the PZT, the normal random error is of the order of 0.18 arc-seconds. This is the internal precision for one night and does not include the effects of longer period phenomena which is probably significantly smaller. It is more difficult to estimate the errors with a longer period. These effects, due to phenomena like the heat island effect of Washington, D.C., the seasonal variation of the heat island effect, and long term weather effects may lead to violation of the horizontal uniformity which is assumed in the normal data reduction procedure. The derivation of the averaged measures for one night at the USNO may be of the order of 0.06 arc-seconds for periods between one and one hundred days.

C. Two-Color Refractometer

In order to address the role of anomolous refraction in these determinations of star position, we suggest the development and use of the Two-Color Refractometer (TCR). The TCR is a system which measures the magnitude of the refraction due to the atmosphere when observing a star. This measurement is not affected by problems of an encoder, a star catalog, or variations in personal equation. It is a measurement which isolates the refraction alone.

The primary subsystem of the Two-Color Refractometer is the Quadrant Sensor System (QSS). The QSS is an operating system which has been developed at the University of Maryland. The QSS is an "eyepiece" which permits one to determine the apparent star position with great accuracy. This determination of the apparent direction to the star is performed by observing in two different colors. Using a knowledge of the index of the refraction and the dispersion of the air, one may compute from this data the instantaneous magnitude of the angle of refraction. Using the local temperature, pressure, and humidity, one may then compute the normal refraction. The difference between the normal angle of refraction and the measured angle of refraction is the anomolous refraction. The latter will be done by exactly the same calculation which is normally used by USNO for the reduction of transit circle observations.

In general, the anomolous refraction will depend upon both zenith distance and time. Let us for the moment neglect the time variation. Then a number of stars may be observed "at one instant" (actually a period of about thirty minutes). The measured value of the anomolous refraction may then be expressed in a power series function about the zenith in terms of "east" and "north" direction. The first term, which will be a constant term, which might be due to the use of erroneous values of local pressure, temperature and humidity, for the computation of the normal refractions. Any linear terms which appear would be due to gradients in the atmosphere. Quadratic terms should be small if the theory is proper and the constant term is not large.

II. OPERATION AND PERFORMANCE OF A QUADRANT SENSOR SYSTEM

In this section we consider an ideal Quadrant Sensor System (QSS) and discuss the expected performance of such a system. The objective of the first part of this section is to define the type of sensor system which would be most desirable and to provide a model for the performance analysis which will appear later in this section. The realization of the QSS system will be discussed in Section IV.

The QSS is based upon a special photosensor, the "Quadrant Photo Sensor" produced by the Electronic Vision Company, a division of Science Applications, Inc. The Quadrant Photo Sensor (QPS) consists of a quadrant silicon diode which is mounted in an evacuated envelope. Photons are converted to photoelectrons at the photocathode and accelerated electrostatically to an energy of 15 KeV. They are then electrostatically imaged onto the quadrant diode. The overall mechanical configuration of the Quadrant Photo Sensor (QPS) is illustrated in Figure 1.

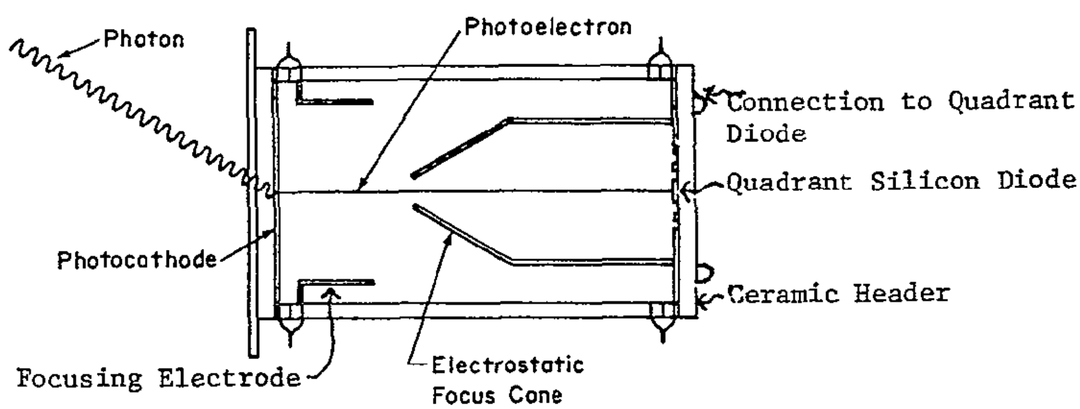

Schematic Diagram of Quadrant Photo Sensor
Figure 1

The photoelectron, which is accelerated to 15 KV, produces extensive ionization within the silicon in the photodiode. The output of a photodiode which is bombarded by a single photoelectron is a charge packet which consists, at the normal operating voltage, of about 2,000 electrons. This pulse signal generated by this charge packet is amplified, shaped, and finally detected with a level discriminator. In order to operate such a system, we wish to provide functions indicated in Figure 2.

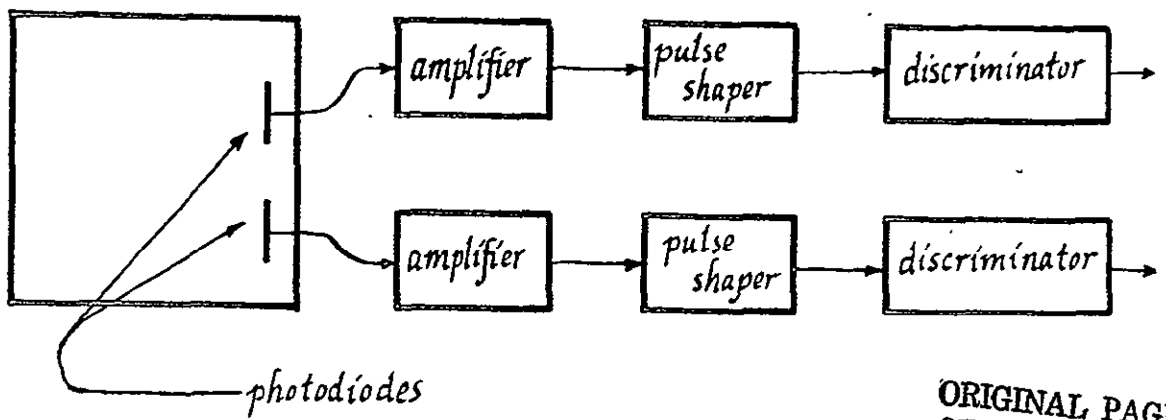

QSS Detection Subsystem for Single Photoelectrons
Two of the Four Channels are Shown
Figure 2

Thus Figure 2 illustrates the photon detection system, which provides a high-level pulse for the arrival of each photoelectron. By accumulating these counts, one would have available the intergal number of counts for any interval. However, we wish to use such a system in several applications where a greater variety of outputs are required. The above system will be used as the basis for the calculations presented in Section II. At present, however, we shall now continue this discussion to describe the full "Quadrant Sensor System requirements. The subsystem described in Figure 2 is connected to a data processing subsystem.

The QSS has been designed both to provide the input for a telescope used for the tracking of stars, but also to detect laser returns from satellites and track on these returns. However, the latter function is not used in this application and will not further be considered.

When operating in the photon sensing mode, the system is expected to produce an output signal which is proportional either to the intergal number of counts or the count rate smoothed in some fashion. Two outputs of this type, which are the difference between the counts from each axis, are available (X high pass, Y high pass). In addition, the output is then filtered with a low pass filter having a time constant of about 1 second. This is available as $X_{\text{low pass}}$ and $Y_{\text{low pass}}$. The high speed outputs will be used as the input for an external subsystem to stabilize the image with a high frequency response. The low frequency output will provide the signals required to move the telescope. The signals described above are available in analog form in order to operate the analog servo-loops. They are also multiplexed onto an A-to-D Converter to provide outputs which may be used for computer control and recording. Thus this unit is capable of both stabilizing the image, and through the photon counts, provide interval number of counts in the various channels.

In this discussion we shall evaluate some of the numerical performance parameters for the quadrant sensor. In this section we shall presume the use of a quadrant photon counting sensor. We will assume that the photocathode has a uniform quantum efficiency and that the electronics system imposes no rate limits. The description of the actual sensor and its limitations appears in a later section.

Photon Noise in Direct Mode

In this section we shall compute the photon noise which affects the determination of the centroid of an image by a Quadrant Sensing System. For pedigogical ease, we shall first consider a stellar image which is square, so the brightness has the form indicated in Figure 3.

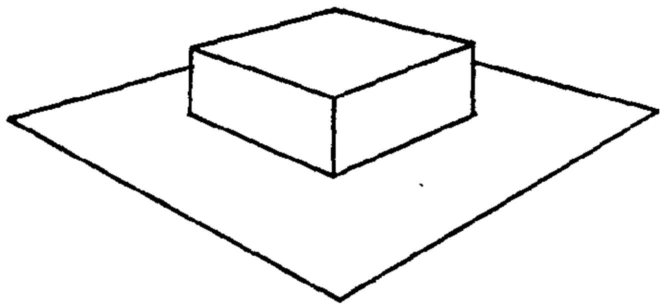

Brightness of Stellar Image
Figure 3

The difference between the performance criteria for this approximation to the stellar image (by a square pillbox) and a more realistic approximation, i.e., a Gaussian or a Lorentzian form, will be discussed later. The more realistic forms will result in about a 2% modification of the numerical results obtained for the square pillbox image.

The results shall be expressed in terms of the total number of photoelectrons which arrive on all four quadrants (denoted by the symbol N) during a time interval denoted by the symbol T. The full width of the image described in Figure 3 is denoted d, which might typically have a value of two arc-seconds for a reasonable telescope used at a good astronomical site. The one dimensional projection of such an image has the form indicated in Figure 4.

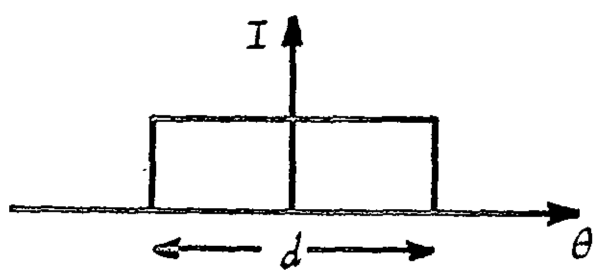

One Dimensional Projection of Square Pillbox Image

Figure 4

The number of photoelectrons per linear arc-second at the center of the square image, denoted by $\tilde{N}$, is given by

$$\tilde{N} = N/d = N/(d_o\sqrt{3})$$

where d_o is the "rms diameter". This quantity is obtained by doubling the rms radius, which is the deviation of the light intensity distribution over the image plane. We may reexpress $\tilde{N}$ in the form

$$\tilde{N} = (\eta N)/(2d_o)$$

where we have defined the symbol η to represent a numerical coefficient which is related to the shape of the image. Thus from the above expressions, we see that for a square image

$$\eta_s = 2/\sqrt{3} = 1.547$$

Now we consider an image with a more realistic profile, i.e., a Guassian. The one dimension projection of such an image is indicated in Figure 5.

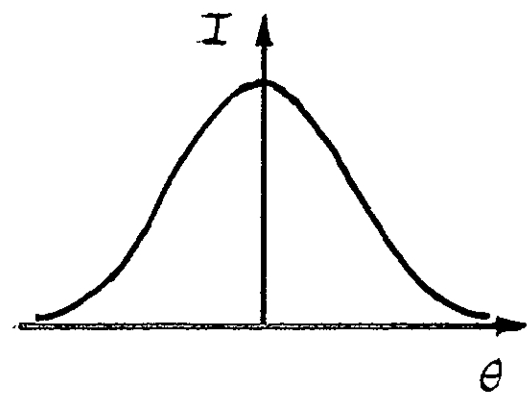

One Dimensional Projection of Gaussian Image

Figure 5

The intensity $\tilde{N}$, expressed as the number of photoelectrons/arc-seconds, has the form

$$\tilde{N}(x) = \frac{\sqrt{2}\ N}{\sqrt{\pi}\ d_o}\ e^{-2x^2/d_o{}^2}$$

Thus at origin

$$\tilde{N} = \tilde{N}(o) = \frac{\sqrt{2}\ N}{\sqrt{\pi}\ d_o} = \eta_g\ N/2d_o$$

Where we have again used the coefficient as η. Thus for the Guassian we have

$$\eta_g = (2\ \sqrt{2})/\ \sqrt{\pi} = 1.5958$$

Thus in general, the value of η will be dictated by the model for the seeing disk, or from a more pragmatic veiwpoint, from an actual measurement of the size and profile of the seeing disk.

We may later take into account a large deflection or error in image position by expressing η as a function of the offset of the image. Thus if there is an average offset of Δ , then η (Δ) will have a smaller value. In this way we will be able to address some problems which will arise in the two color application. Thus for a Guassian image

$$\eta\ (\Delta) = \frac{2\sqrt{2}}{\sqrt{\pi}}\, e^{-2\Delta^2/d_o^2}$$

The quantity $\tilde{N}$ is physically related to the change in signal or differential count rate for motion of the image. Thus if we apply a sinusoidal offset or a "dither" to the position by an optical device, we will see a similar variation in $\tilde{N}$. This will obviously be related to the profile, as expressed by η. On the other hand, if we assume a profile, we may invert this relation and use the measured value of $\tilde{N}$ which is obtained by applying a dither to the servo-system to evaluate the seeing disk diameter, using the expression

$$d_o = \eta\ N/2\tilde{N}$$

If the image is nominally centered, then a small image offset which is parameterized by the value of θ will result in a difference in count rates which is given by:

$$\Delta N = N_L - N_R = (N_{Lo} + \tilde{N}\cdot\Theta) - (N_{Ro} - \tilde{N}\cdot\Theta)$$

We will describe the one-dimensional case. If the image was initially centered and the quantum efficiencies of the effective areas of the photocathode are equal then $N_{Lo} = N_{Ro}$ and the above equation becomes

$$\Delta N = 2\tilde{N}\Theta = \eta\ N\Theta/d_o$$

which may be reexpressed as

$$\Delta N/N = \eta\ \Theta/d_o$$

or using ΔN to compute the offset angle

$$\Theta = (\Delta N/N)\ d_o/\eta$$

We may now define a relative angle which is expressed in terms of the image diameter, so we have

$$\alpha \equiv \Theta/d_o = \Delta N/N\eta$$

This expresses the angular offset due to an inequality in counts as a dimensionless angle.

Now let us determine the standard deviation of the angular position due to shot noise, i.e., the statistical error in the determination of the centroid due to the photon statistics. In each pair of quadrants (presuming we sum the photocounts from both quadrants of each side to determine the error) the mean value is

$$\bar{N}_L = \bar{N}_R = N/2$$

Thus for large values of N, the statistical noise in the value of each of these is

$$\delta N_L = \delta N_R = \sqrt{N/2}$$

Since the statistical noise in each of these quantities are independent, we have

$$\delta N = \sqrt{(\delta N_L)^2 + (\delta N_R)^2} = \sqrt{N}$$

inserting this value of δN into the above expression for α yields an equivalent angular offset due to the noise. Thus we have

$$\alpha = 1/\eta \sqrt{N}$$

At this point, these considerations will be extended to include the effect of a uniform sky background on the performance. Thus the presumed brightness now takes the form

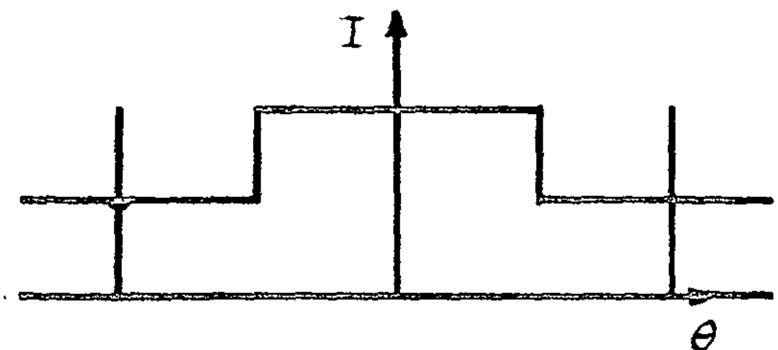

Brightness Distribution for Sky Background With Boundary of Photosensitive Region Marked

Figure 6

where N_b is the total number of counts which appear in the four quadrants due to the brightness of the background sky. This is equal to the product of the field of view (in arc-seconds), the background illumination (in photoelectrons/arc-second/sec), and the integration time (in seconds). The product is expressed in photoelectrons. The image of the star is characterized as in the previous discussion. In this treatment, one simply adds the background to the image, so the mean number of counts on each side is given by

$$N_L = N_R = (N + N_b)/2$$

Thus the photon shot noise in one of the pairs of quadrants (again for relatively large signals) is given by:

$$\delta N_L = \sqrt{N_L} = \sqrt{(N + N_b)/2}$$

and the values for N_R and δN_R have similar expressions. Now if we take the difference of these two independent qualities and use this quantity to determine the apparent error in pointing angles, with the presumption that the photon statistics on the two sides are independent and the sky illumination is spacially uniform, we have

$$\Delta N = \sqrt{N + N_b}$$

Thus for α we have

$$\alpha = \sqrt{N + N_b}\big/\eta N = \sqrt{1 + (N_b/N)}\Big/\eta\sqrt{N}$$

where we have used the total counts for the noise in the numeration, and the counts in the image for the signal which appears in the denominator. We have two types of behavior of interest, the first of which consists of the case when the background is negligible. For this case the error becomes

$$\alpha = 1/\eta\ \sqrt{N}$$

as discussed earlier. This is illustrated for the case of a Gaussian image in Figure 5 by the solid line.

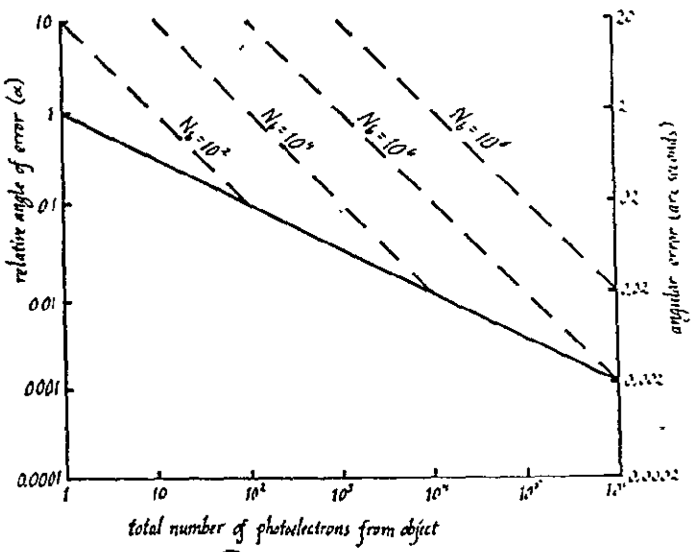

Figure 7.

The other extreme case is when there is a high level of background illumination. This might represent observations conducted in the daytime with a blue sky. In this case we have:

$$\alpha = \sqrt{N_b/N} \Big/ \eta\sqrt{N} = \sqrt{N_b} \Big/ \eta N$$

This may be summarized in graphical form by the dashed line in Figure 7.

Thus Figure 7 indicates the performance that one may expect to obtain with the quadrant sensor. The expected error in the relative angle and the expected error in arc-seconds, presuming a seeing disc diameter of two arc-seconds are related to the total number of photoelectrons received during the observation period.

We may now transform this relationship to describe the behavior with respect to stellar brightness and telescope aperture. Let us, for example, consider a 48-inch telescope and photoelectron count rates which are caused by a particular stellar brightness for a G-2 star (or solar reflection from a satellite). We assume a quasi- S-20 photocathode as measured for a tube of this type and six mirrors with reflectivities of 0.7, 0.7, 0.86, 0.86, 0.86, and 0.86. Thus for the case of a Guassian image with negligible sky background we have the relation indicated in Figure 8.

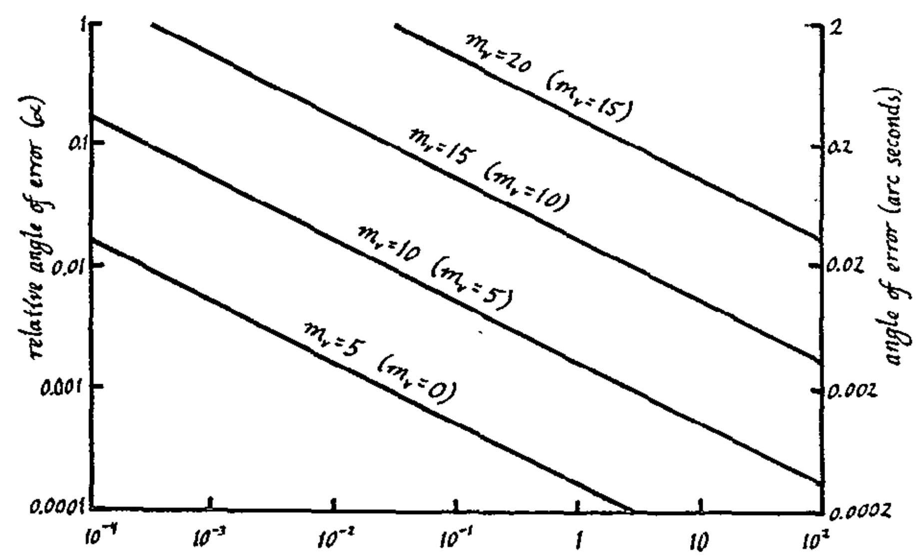

Figure 8.

This indicates the ability to go to rather faint objects and still have very small angular errors due to the photon counting. The numbers in parentheses indicate the results for a 4.8-inch aperture.

III. TWO COLOR APPLICATIONS

The Quadrant Sensor System, as a component of the Two-Color Refractometer system may be used to obtain high accuracy measurements in absolute astrometry. In particular, it will determine the deviation in the apparent star position caused by the earth's atmosphere. As star light enters the earth's atmosphere, the deviation of index of refraction of the atmosphere from that of the vacuum results in a change in the direction of propogation. For a flat, horizontally-stratified atmosphere, this change in direction is a known function of the index of refraction of the air in the immediate vicinity of the telescope (the local index of refraction). This may be determined from the local temperature, pressure and humidity. However, if there are horizontal inhomogeneities, this change of propogation direction can not be predicted from a measurement of local surface conditions. In this section, we address a procedure to determine the magnitude of this change in direction (the "angle of refraction") from measurements made on the light of the star using the Quadrant Sensor System.

We take advantage of the fact that the magnitude of the angle of refraction depends upon wavelength, due to the dispersion of the index of refraction of air. Thus by measuring the apparent position of the star as viewed in red and in blue light, the difference in apparent position may be evaluated. This dispersion angle may be used with a knowledge of the dispersion in the index of refraction to determine the angle of refraction. Thus using the dispersion angle between the red and blue images, and the known dispersion of the air, we may determine the deviation of the direction of propogation of the starlight due to the atmosphere.

In order to illustrate the operation of the Two-Color Refractometer (TCR) let us consider the basic relations governing the refraction. The symbol Θ_λ describes the deviation of a ray of wavelength λ from its initial direction and ϕ is the true zenith distance of the star. The index of refraction of the air at the wavelength λ is denoted by η_λ. Thus from Snell's law, we have

$$\Theta_\lambda = (\eta_\lambda - 1)\phi/\eta_\lambda$$

Since η_λ is very close to unity, we shall approximate this expression by:

$$\Theta_\lambda = (\eta_\lambda - 1)\ \phi$$

where the definition of these quantities may be seen in the following figure

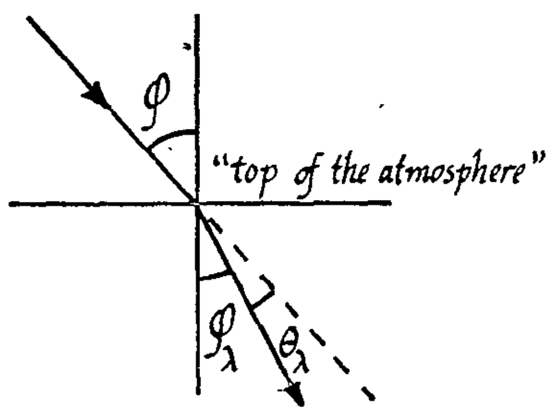

Effect of Refraction on Starlight
Figure 9.

While the figure illustrates a simple idealized case, a little reflection indicates that equations apply to the more general case of a continuously variable, non stratified, spherical atmosphere. For the calculation made in the later part of this section, we use the following expression for the index of refraction for dry air

$$(\eta_\lambda - 1) \times 10^{-6} = 64.328 + 29498.1\ (146 - \lambda_0^{-2})^{-1} + 255.4\ (41 - \lambda_0^{-2})^{-1}$$

This applies for a temperature of 15°C, a pressure of 760 mm and no water vapor. This expression is not the optimal form for expressing the index of refraction when reducing the data for the operational system, but it is entirely satisfactory for the system analysis and error analysis presented in this section.

In order to permit the independent variation of the wavelength selected for observation within a reasonable error analysis, we shall use the blue and red measurements and a parameter which depends on the wavelengths used to determine the magnitude for the angle of refraction at a reference wavelength chosen to be the center of the visual band (5600Å). Thus for the wavelengths at which we will measure the relative angular position, we use:

$$\Theta_R = (\eta_R - 1)\phi$$

$$\Theta_B = (\eta_B - 1)\phi$$

We will then use these expressions to determine the zenith distance φ, which we will relate to the angle of refraction in the green by the relation

$$\Theta_V = (\eta_V - 1)\phi$$

Thus we will determine the angle of refraction in the visual band. This particular equation does not appear to represent the optimal procedure for minimizing thd propogation of experimental errors but we shall use it as a useful tool for system analysis. Thus we obtain an expression of the form:

$$\Theta_V = \Omega\ (\Theta_B - \Theta_R)$$

where

$$\Omega = (\eta_V - 1)/[(\eta_B - 1) - (\eta_R - 1)]$$

If we measure the difference in apparent angular position of the blue and the red image, this angular difference, multiplied by the quantity Ω, will yield the angle of refraction suffered by the visible light. This is the value for local conditions which are 15°C and a pressure of 760 mm Hg.

In order to provide a general frame of reference, let us consider the numerical values for the refraction and the dispersion angles. Let us consider the value of Ω for various choices of the limiting wavelengths. We have

Effective Blue Wavelength	Effective Red Wavelength	Ω
3500Å	6000Å	30.36
3300Å	6000Å	25.27
3500Å	7000Å	26.89

Relation Between Selected Wavelengths and Ω Multiplier

Table 1

Since the eventual error is proportional to the value of Ω, we would prefer the smallest possible value. From Table 1 we see that the value of Ω decreases and thus the error multiplier decreases as the spread between the wavelengths increase. This dependence is particularly sensitive to the wavelength of the blue observation where a change of 200Å provides as much improvement in Ω as a change of 1000Å in the wavelength of the red observation. However, for various technical reasons we will accept the first case as a reasonable, practical limit.

Let us now evaluate the sources of error in this determination. Differentiating the expression for Θ_V, we have:

$$\delta\Theta_V = \frac{\delta\Omega}{\Omega}\Theta_V + \Omega\,(\delta\Theta_B - \delta\Theta_R)$$

We now presume the uncertainty in the measurement of the angular position of the image in the red and in the blue have the same magnitude, and are independent. Concerning the former, it assumes similar filter widths which will probably not be the case, but it is a useful point for discussion. Thus for the part of the variation due to uncertainty in angular measurement we have

$$\delta\Theta_V \quad \sqrt{2}\ \Omega\ \delta\Theta$$

where

$$\delta\Theta = \delta\Theta_B = \delta\Theta_R$$

We may now use the relations between the total number of counts and angular errors to express the accuracy of the determination of $\delta\Theta_V$ as a function of the total number of photoelectrons. In Figure 10 we have also indicated the various system operating points obtained when the QSS is running at the maximum count rate (the normal procedure) for various intervals of time. These results include the effect of the UV filter and the red filter.

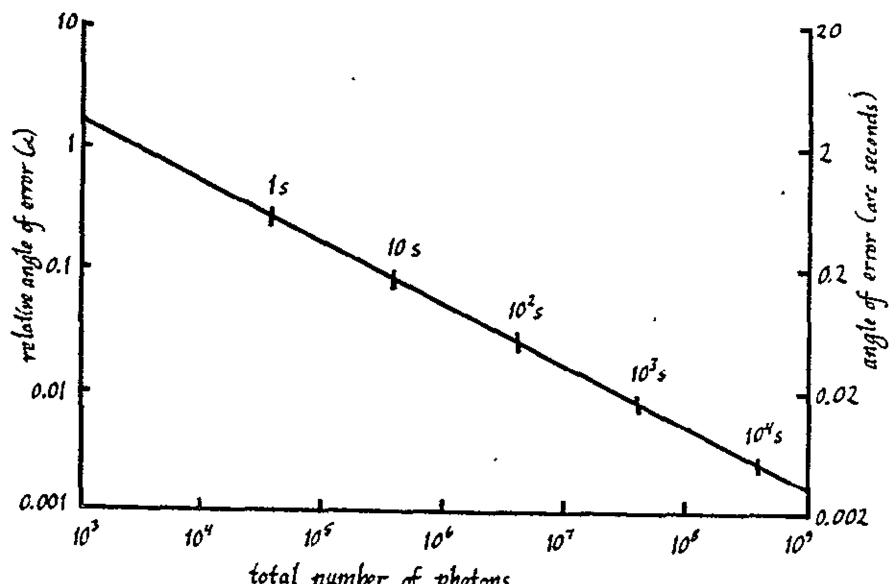

Relation between total number of counts and error in anomalous refraction for TCR.

Figure 10

We now consider the other source of error which appeared in the Equation for $\delta\Theta_V$. This is the possible variation in the quantity Ω. It is presumed that Ω is calculated for the local value of refraction (i.e. using pressure and temperature). The predominant remaining reason for an uncontrolled uncertainty in $\delta\Theta_V$ is due to the variable water vapor content in the atmosphere. In order to evaluate this phenomenon, the following table is presented. This presents the value of Ω and the change produced in Ω due to precipitable water for various pairs of effective wavelengths. We use the mean water vapor which is expressed in the terms of precipitable water vapor (for a flat atmosphere).

Effective Wavelength for Blue Filter	Effective Wavelength for Red Filter	Ω for no Water	Precip-itable H_2O	Ω with Water Vapor	$\delta\Omega/\Omega$
3500	6000	30.3657	10 mm	30.1885	0.0058
3300	6000	25.2696	10 mm	25.1232	0.0058
3500	7000	26.8927	10 mm	26.7351	0.0059
3500	6000	30.3479	1 mm	---	0.00065

The Effect of Water Vapor on Systematic Errors
Table 2

Thus we see that the water vapor correction is approximately proportional to the amount of water and generally independent of the selection of the effective wavelength of the filters.

Let us now consider a numerical example. If we observe a star at zenith distance of 30° as one might with an astrolabe, then using the expression for the refraction under standard temperature and pressure

$$\Theta_V = 58''.2 \tan Z$$

which applies to a flat atmosphere we have, at 30° a deflection of about 34". If we wish to be able to determine this correction with an accuracy of 0"05, then we need

$$\frac{\delta\Theta_v}{\Theta_v} = \frac{\delta\Omega}{\Omega} = \frac{0''05}{33''6} = 0.0015$$

This means one to know the water content to 2.3 mm of precipitable water.

However, this requirement is not particularly difficult since commercially available microwave radiometers are accurate to about 1 or 2 mm of precipitable water. In addition, a system ttached to the TCR using near IR measurements in and out of a water absorbtion band should be significantly more accurate and less complicated.

Some Practical Considerations

We now consider a few practical aspects of the design of the TCR. The full discussion of the system will be considered at a later time.

We first consider the procedure for sampling the light at two different colors. One might attempt to measure the position of the red and blue images at the same time with two different quadrant sensors. The parameters which enter Figure 6 are based upon this assumption. However, a more practical approach to this problem is to use a single quadrant sensor. The detailed reasons will be considered in a separate discussion. We shall, briefly, discuss this approach and how we should use it to maximize the accuracy of the evaluation. Thus we note that due to the fact that the refraction in the atmosphere has significant power at various frequencies, one might wish to sample the two different colors continuously and at the same time. If this is done, then both the power at high frequency and the power at low frequency (the image motion) are properly tracked and do not affect the accuracy of the measurement.

However, the mechanical stability requirements strongly suggest the use of a single detector. If one switched the two colors onto the one sensor at a rate of several hundred times a second, one may show that the residual error is expected to be random and has a value of less than 0.01 arc-seconds for a measurement lasting several minutes.

The remaining uncertainty is in the determination of the water vapor. From the previous discussion, and typical values of water vapor to be expected, this effect may be totally ignored for the initial measurements out to a distance of 15° from the zenith.

Expected Accuracy for Measurements of Zenith Refraction

We now discuss the accuracy which we would expect to obtain with measurements using this instrument. These will be expressed in terms of the measurement errors to be expected on the power spectral density, and will be based upon use of the 48-inch telescope at the Goddard Optical Research Facility (GORF). However, approximately the same numbers apply to the set of measurements which would be performed on the 36-inch telescope. For these evaluations, we will presume the use of the present circuit for the quadrant sensor which has a maximum counting rate of 10 kilohertz/quadrant. This will permit the observation of 8th magnitude stars with the proper count rate. Since we will limit our measurements to a region that is between 5 and 10 degrees, it is worth noting that we would statistically expect to have about 80 stars within a five degree circle of the zenith.

In general, the relationship between the stellar magnitude, the telescope aperture and the expected photon statistical error for a ten minute observation is expressed in Figure 11.

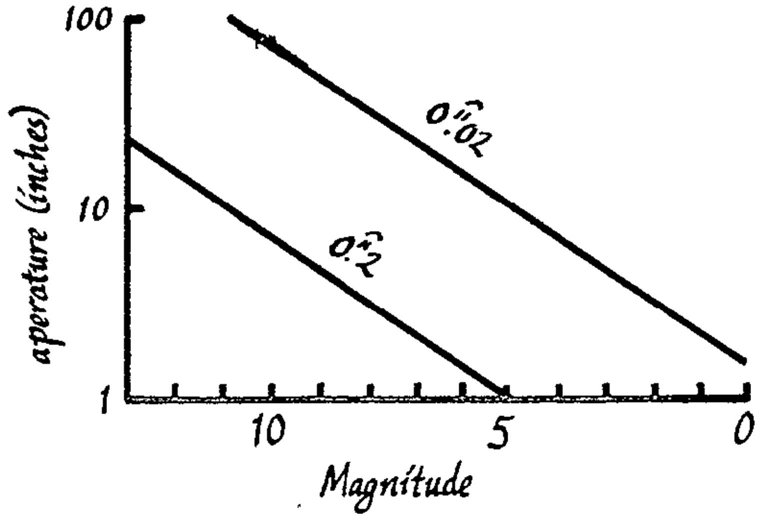

ORIGINAL PAGE IS
OF POOR QUALITY

Figure 11

Combining the results of Figure 10 and Figure 11, we see that we may trade off between the aperture size of the telescope with the observing time to use a small telescope and still have a reasonable number of stars to observe.

Now presuming this count rate, we can evaluate the power spectrum of the system errors which we expect. To facilitate this present discussion, we will not consider the true power spectrum but indicate the standard deviation of the system error for a measurement of a given length. The overall results are thus summarized in Figure 12. The system error caused by the photon statistical noise is illustrated by the broad solid line. For periods shorter than one second, one may increase the centroid of the white light image and rely on the smoothness of the telescope tracking to determine the refraction (called image in this domain) rather than the two-color extraction. This is expected, with some study of the records and knowledge of the telescope, to give about 0.″2. If these measurements were conducted on the 100-inch telescope at Mt. Wilson, which has a very smooth and regular drive, and were conducted on a night of low wind, this system error could probably be reduced to 0.1 arc-seconds. For periods of more than 10 seconds, however, one would expect that errors in the telescope drive will become too large. In order to study the behavior for longer characteristic times, we consider a limit for a single observation of twenty minutes which results in an error of 0.01 arc-second. Thus one might expect to obtain an increase in accuracy by about a factor of three, but this will mean the observation of new stars. The feasible accuracy in this region must be more carefully explored. For the longer period term, one averages the data obtained on successive nights to obtain these results. However, since we do not expect to observe for 24 hours a day, there is a break in this curve as one goes to the dashed portion. Presuming an observation period of two hours for a night, we obtain the dashed curve. At about 0.03 arc-seconds one expects to run into systematic errors. It seems possible that these may be calibrated to the 0.001 or 0.002 arc-second level. Accuracies beyond this cannot currently be projected for the first generation instrument.

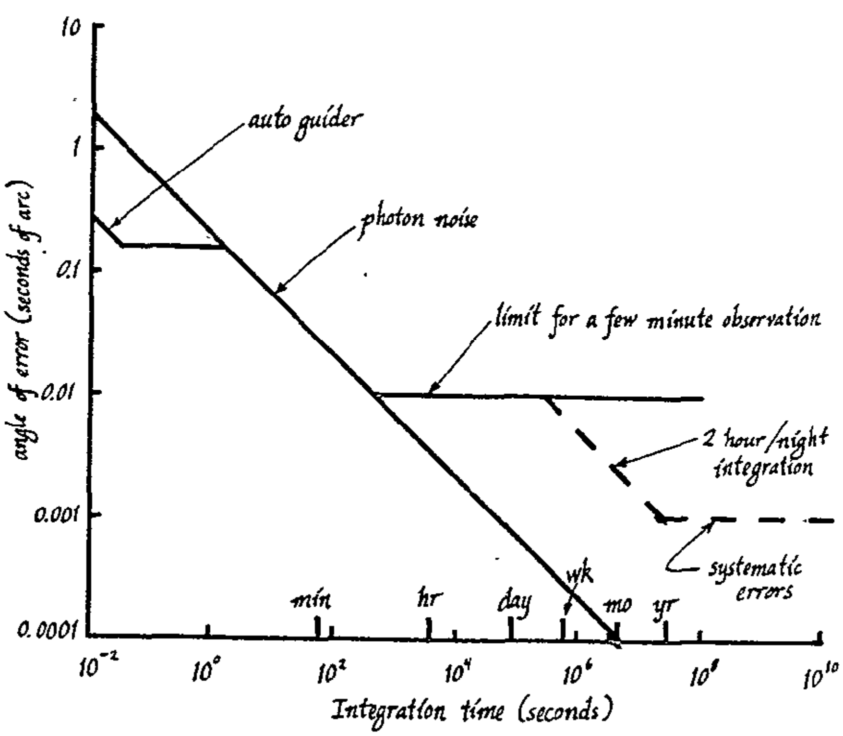

Figure 12

IV. IMPLEMENTATION OF THE QUADRANT SENSOR SYSTEM

In this section we describe the Quadrant Sensor System which has been developed within the Amplitude Interferometry Program at the University of Maryland. This system is the practical realization of the hypothetical QSS which was described in Section II. The basic element of the system consists of two standardized units, the photo-sensor head and the control unit which have been used in three different astronomical systems. The quadrant sensor system is basically a special system which detects light in four channels. These are closely placed and are mechanically and geometrically rigid. In order to satisfy the system requirements, a special device has been obtained from the Electronic Vision Company and an electronic system has been developed at the University of Maryland to make these observations. The requirements on this optical/electronic system demand a very high precision, electronically, optically, and mechanically, as well as a considerable amount of generality. The electronic system will permit the quadrant sensor to interface to a variety of data processing systems, i..e, computers or hardwired processors.

The Photosensor head contains the Quadrant Photisil. The structure has already been indicated in Figure 4 and is shown here

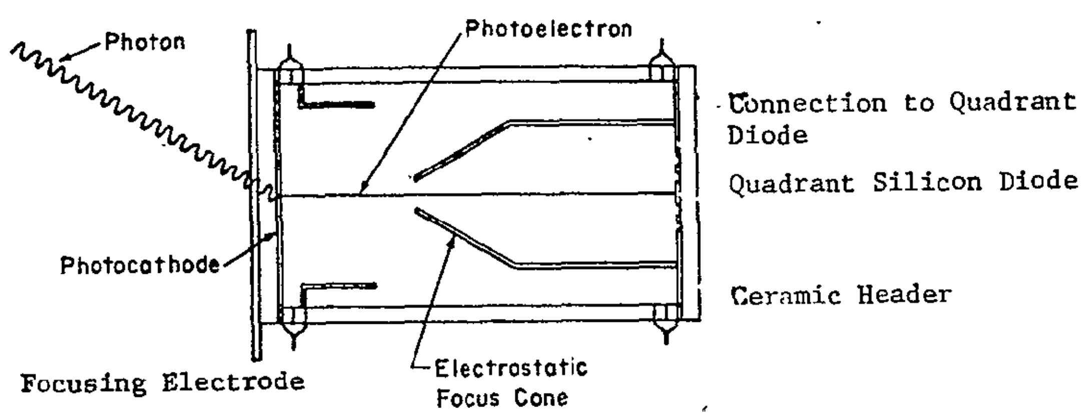

Schematic Diagram of Quadrant Photo Sensor

Figure 13

As discussed in the first section, the circuitry following the Quadrant Photosil is indicated in Figure 14.

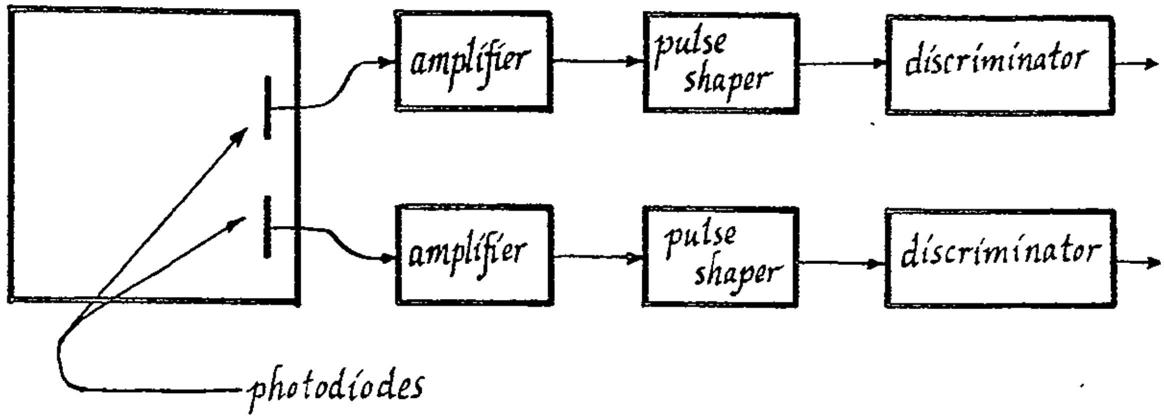

QSS Detection System for Single Photoelectrons
Two of the Four Channels are Shown
Figure 14

This results in a pulse height distribution which permits a straightforward discriminator. The preamplifier is similar to that photon counting Digicon system developed by E. Beaver at UCSD. The pulse height distribution at 16 KV is shown in the following figure.

ORIGINAL PAGE IS
OF POOR QUALITY

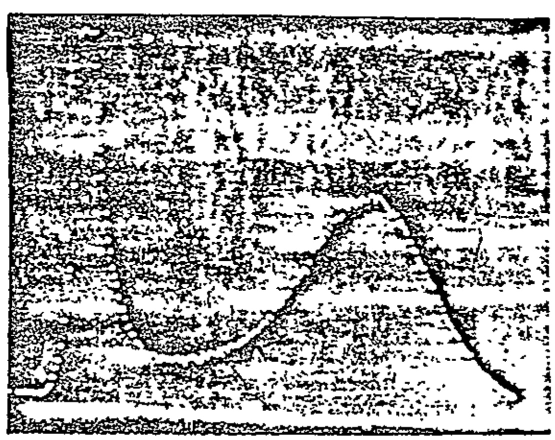

Figure 15

This system is expected to operate in environments with high levels of external EMI. This is a serious problem since the signals are smaller than conventional PMT's by a factor of about 1000 to 10,000.

Special shielding and grounding procedures are required in order to prevent external TVI from interfering with the discrimination process. This has been provided for the input high voltage leads by the use of solid aluminum shields. The amplifiers are specially isolated and grounded. Even so, the pickup is noticable under certain circumstances.

The preamplifier in the QSS head provides a signal which is relatively immume to external problems. This is then sent by four short cables to the QSS Control Unit. Here the signal is reamplified and sent to discriminators. These discriminators may be adjusted independently for each of the four channels. These are normally set at about the point indicated by the arrow in Figure 15. The shape of this pulse height distribution leads to a relative immunity from effects due to the variation one expects in operating voltages and circuits in the field.

In order to interface to a computer and provide data for the closure of a servo-loop, the four signals are multiplexed and then applied to an A-to-D converter. The output is an eight-bit word. The operation acts as an asynchronous peripheral which supplies data when asked. Thus the output of the ADC is available as a digital signal. This generalized system has been used in several applications. We shall now describe how it has already been used.

<u>Application in Single Aperture Amplitude Interferometer</u>

The first application of the quadrant sensor system was to provide image stabilization in Single Aperture Amplitude Interferometry (SAAI). In this system it operates in only one axis. It incorporates a device which provides high frequency stabilization with a frequency response up to about 60 hertz. The gain is set to permit the utilization of the stabilization to this level. The expected noise performance was discussed in the previous section.

As an indication of the proper performance of this system in Amplitude Interferometry, the measurements of the fringe visibility which are performed when this system is operating are significantly improved. Special procedures have been developed, both for the proper alignment of this system and to permit the simultaneous use of the manual guiding of the telescope. This is required at present since the QSS has not yet been interfaced to the large telescopes due to the necessity of performing the coordinate transformation without a computer.

48-inch Telescope at the Goddard Space Flight Center

The Quadrant Sensor System (QSS) has been used to make an Automatic Guider System (AGS) to control the 48-inch telescope at the GORF. In this case, the output from the high frequency error signal is multiplexed and digitized and fed directly to the computer. There this data on the error in pointing is processed and filtered in a digital form. This system has succeeded in providing precise pointing information and also has been useful in detecting difficulties in the encoder system. Instabilities in the computer processing of the data and the telescope setup drive can cause oscillation under some circumstances. However, the computer procedure for handling the data is now being reprogrammed to handle this properly.

In addition, the GSFC system also provides for the capability to sense the offset of lasers from a satellite reflection. To this end, the capability is provided to gate the photocathode off while the outgoing laser pulse is near the telescope with a high voltage pulse applied to a grid of a modified Quadrant Photosensor. The sensor system can detect the arrival of a laser return. The signal on each diode is amplified, and then compressed for greater dynamic range, and stores before it is presented to the multiplexer. This sequence is activated by the receipt of a photo pulse which has a value which is greater than three photoelectrons. Thus this gives the error in pointing with respect to the laser return. This system has been implemented and tested in a laboratory but the required computer programs for the 48-inch telescope and the required telescope time are not yet available in order to test the laser tracking system on the telescope.

APPENDIX II

ON THE USE OF WIDEBAND OPTICAL VERY LONG BASELINE INTERFEROMETER FOR THE DETERMINATION OF THE POSITION OF THE POLE

On the Use of

Wideband Optical Very Long Base Line Interferometer

for the

Determination of the Position of the Pole

Local Reference Frame

The discussion of the stellar measurement and the atmospheric correction have related the reference points on the piers to the stellar frame. Let us now consider the relation of these two points to the earth. They are set into concrete piers which are buried in the mountain. The questions concerning these reference points are:

1) The piers may move with respect to the local ~~geological~~ formations.

2) The local formation may move (distortion of the shape of the mountain).

3) The mountain may move with respect to surrounding terrain.

4) Continental drift may be moving the observatory.

5) Polar motion changes the declination.

These possible motions are all "problems" but they also represent phenomena of geophysical interest. The primary difficulty is when all these motions occur simultaneously, so that it is difficult to evaluate them separately from the declination measurements. To this end, three methods may be used to relate the reference points to the earth. These are:

A) Piers—the piers tie the reference points to the local geological structure.

B) Local Gravity Vector—the reference points (and the declination angle) may be tied to the local gravity vector.

C) Distant References—the reference points may be related to piers over a distance of about 10 kilometers, forming a net of local references.

Thus the large scale motion may be separated from possible local motion and changes in the direction of the local gravity vector.

Douglas G. Currie
30 December 1971

On the Use of

Wideband Optical Very Long Base Line Interferometer

for the

Determination of the Position of the Pole

Atmospheric Correction by the Use of Dispersion

The following is a description of a procedure to eliminate the effects of the atmosphere as a source of systematic error in the use of a Wideband Optical Very Long Base Line Interferometer (WOVLBI). It uses the very high resolution intrinsically available with the WOVLBI to determine an atmospheric correction in a manner similar to the method used in the two-color laser distance measurements. The correction in stellar declination is accomplished by measuring the apparent declination of a star at two different wavelengths. The difference in apparent angle between these two measurements is then used to determine the magnitude of the total refraction correction. The accuracy of the declination measurement which results from the use of this procedure is by a factor of 30 less than the intrinsic angular resolution. However the extremely high angular resolution available with a WOVLBI system permits an accuracy of 20 cm or better on the polar position.

In general, when the declination of a star is measured, the refraction in the atmosphere results in an offset of the measurement. For observations made near the zenith, measurements of the local pressure and its horizontal gradiant may be used in a quasi-static model of the atmosphere to make corrections to about 0".005. However, dynamic effects in the atmosphere (winds) may cause deviations from the quasi-static model which, at the worst type of observing site, could be as large as 0".1.

However, the extremely high resolution (0".00008) of the WOVLBI makes available a method which does not require the meteorological monitoring. To illustrate this method, let us consider the index of refraction of the atmosphere as a function of wavelength, for a particular pressure and temperature. This may be represented by

$$n(\lambda) - 1 = 0.000288 \left\{1 - \left(\frac{0.0751\mu}{\lambda}\right)^2\right\} = \alpha \left\{1 - \left(\frac{\lambda_d}{\lambda}\right)^2\right\}$$

This expression may be used to obtain the difference in the index of refraction for two separate wavelengths. This may be approximated by (where $\lambda_a < \lambda_b$)

$$\Delta(\lambda_a,\lambda_b) \equiv \frac{(n(\lambda_a)-1) - (n(\lambda_b)-1)}{\frac{1}{2}[(n(\lambda_a)-1)+(n(\lambda_b)-1)]} \approx \left(\frac{\lambda_b}{\lambda_a}\right)^2 \left\{1 - \left(\frac{\lambda_a}{\lambda_b}\right)^2\right\}$$

The choice of the critical short wavelength, λ_a, (which essentially determines the degree to which the resolution is degraded in obtaining the refraction correction) is limited by the absorption of the atmosphere. Thus we choose 3500 Å as the center of the short wavelength passband. For the long wavelength passband, the limit is set by the decreasing sensitivity of the photocathode of the photomultiplier. However, correction factor is rather insensitive to this choice, and we will presume a passband centered at 6500 Å, so we have

$$\Delta \equiv \Delta(3500\ \text{Å},\ 6500\ \text{Å}) = 0.0324 \approx \frac{1}{31} \left(\frac{0.35\mu}{\lambda_a}\right)^2$$

The above expression describes the properties of the atmosphere. Let us now relate this to the WOVLBI measurements and their correction. Basically, a VLBI-type measurement (either radio or optical) measures the range to the object of interest from two different reference points on earth. While these measurements are normally converted to an angle for discussion, the analysis of the atmospheric effects may be more effectively carried out in terms of the range.

Between each reference point and the star, the light passes through a part of the atmosphere. Thus for the path to each reference point, there is an atmospheric contribution to the range due to the fact that the index of refraction of the atmosphere is not equal to unity. This deviation in the path length, ℓ_1 and ℓ_2 for the two reference points is given by

$$\ell_1 = \int_0^\infty \{n_1(\ell,\lambda) - 1\}\ d\ell$$

where n depends upon ℓ due to the changes in density, temperature and composition along the path from reference point 1 to the star. If we assume that the variation of composition along the path has a negligible effect (the primary component, water vapor, indeed has a very small effect) then the only change in (n − 1) is a multiplicative constant and we may separate the density and wavelength dependence in the form

$$\ell_1 = \int_0^\infty \frac{\rho_1(\ell)}{\rho_o} \{n(\lambda) - 1\} \; d\ell$$

$$= \{n(\lambda) - 1\} \int_0^\infty \frac{\rho_1(\ell)}{\rho_o} \; d\ell = \{n(\ell) - 1\} R_1$$

where R_1 is defined as

$$R_1 \equiv \int_0^\infty \frac{\rho_1(\ell)}{\rho_o} \; d\ell$$

The zero order fringe is deviated from its proper position (the position in the absence of the atmosphere). Thus for one particular wavelength, the offset, $\Delta\ell(\lambda)$, due to the atmosphere is

$$\Delta\ell(\lambda) \equiv \ell_1(\lambda) - \ell_2(\lambda) \doteq [n(\lambda) - 1] \; (R_1 - R_2) \; .$$

Now considering the zero fringe position for two different wavelengths, we have, for their separation

$$\delta\Delta\ell \equiv \Delta\ell(\lambda_a) - \Delta\ell(\lambda_b) = \{[n(\lambda_a) - 1] - [n(\lambda_b) - 1]\} \; (R_1 - R_2)$$

Knowing $n(\lambda)$, we may solve for $(R_1 - R_2)$ and define

$$\bar{\lambda} \equiv \tfrac{1}{2}(\lambda_a + \lambda_b)$$

we have

$$\Delta\ell(\bar{\lambda}) = [n(\bar{\lambda})-1] \; [\delta\Delta\ell]/[(n(\lambda_a)-1) - (n(\lambda_b)-1)] = \delta\Delta\ell/\Delta$$

The quantity $\delta\Delta\ell$ is the observationally measurable quantity, the linear difference between the positions of zero phase difference. One then multiplies by 31 to obtain the total correction required. In the same manner, the uncertainty in determining $\delta\Delta\ell$ or the uncertainty in measuring the position of the zero fringe is multiplied by 31 so the accuracy is less than the intrinsic instrumental resolution.

Douglas G. Currie
27 December 1971

Publications

INTERACTION CONTRA CLASSICAL RELATIVISTIC HAMILTONIAN PARTICLE MECHANICS, Jour. Math. Phys. 4: 1470 (1963).

RELATIVISTIC INVARIANCE AND HAMILTONIAN THEORIES OF INTERACTING PARTICLES, Rev. Mod. Phys. 35: 350 (1963) (With T. F. Jordon and E. C. G. Sudarshan).

N-QUANTUM APPROXIMATION OF THE Λ^4 THEORY, Bull. Am. Phys. Soc. 9: 449 (1964), (with O. W. Greenberg).

ON "DIAGONAL" COHERENT STATE REPRESENTATIONS FOR QUANTUM MECHANICAL DENSITY MATRICES, Jour. Math. Phys. 6: 734 (1965) (with J. R. Klauder and J. McKenna).

A NEW CLASS INVARIANCE TRANSFORMATIONS IN CLASSICAL HAMILTONIAN PARTICLE DYNAMICS, Ann. Phys. 36: 104 (1966).

RELATIVISTIC CONTRIBUTIONS TO LANDAU DAMPING, Phys. of Fluids 9: 1423 (1966) (with R. Aaron).

POINCARE INVARIANT EQUATIONS OF MOTION FOR CLASSICAL PARTICLES, Phys. Rev. 142, 817 (1966).

Q-EQUIVALENT PARTICLE HAMILTONIANS, I. THE CLASSICAL ONE-DIMENSIONAL CASE, Jour. Math. Phys. 7: 967 (1966), (with E. J. Saletan).

ONE DIMENSIONALITY OF RELATIVISTIC PARTICLE FORCES FOR UNIFORM CENTER-OF-MASS MOTION, PRL 16: 1210 (1966), (with E. J. Saletan).

PARTICLE POSITION IN SCATTERING THEORY, Bull.Am. Phys. Soc., 11: 352 (1966).

PROPERTIES OF Q-EQUIVALENT HAMILTONIANS, Bull. Am. Phys. Soc., 11, 372 (1966) (with E. J. Saletan).

INTERACTIONS IN RELATIVISTIC CLASSICAL PARTICLE MECHANICS, Summer Institute for Theoretical Physics 1967, Gordon and Beach Science Publishers (New York) (with T. F. Jordon).

CONSERVATION OF MOMENTUM AND ANGULAR MOMENTUM IN RELATIVISTIC CLASSICAL PARTICLE MECHANICS, Phys. Rev. 167, 5, (1968) (with T. F. Jordon).

SOME IMPLICATIONS FOR PHYSICS AND GEOPHYSICS OF LASER RANGE MEASUREMENTS FROM EARTH TO A LUNAR RETRO-REFLECTOR, Proceedings of the N.A.T.O. Advanced Study Institute on "The Application of Modern Physics to the Earth and Planetary Interiors", edited by S. K. Runcorn, published by Wiley Publishing Co., 1968 (with C. O. Alley, P. L. Bender, R. H. Dicke, J. E. Faller).

SATELLITE GEODESY USING LASER RANGE MEASUREMENTS ONLY, Journal of Geophysical Research 73, 5353 (1968) (with C. O. Alley, P. L. Bender, and J. E. Faller).

LASER BEAM POINTING TESTS Surveyor VII Mission Report, Part II, Science Results NASA TR-32-1264 (with C. O. Alley).

Publications Continued

LASER BEAM POINTING TESTS Surveyor Project Final Report, Part II, Science esults NASA TR-32-1265 (with C. O. Alley)

ON THE ATMOSPHERIC PROPERTIES AFFECTING AN AMPLITUDE INTERFEROMETER NAS-NRC Wood's Hole Summer Study on Synthetic Aperture Optics, 1968.

ON A DETECTION SCHEME FOR AN AMPLITUDE INTERFEROMETER NAS-NRC Woods Hole Summer Study on Synthetic Aperture Optics, 1968.

LASER RANGING RETRO-REFLECTOR AND APOLLO 11 PRELIMINARY SCIENCE REPORT, NASA SP-214 (1969).

APOLLO 11 LASER RANGING RETRO-REFLECTOR: INITIAL MEASUREMENTS FROM THE McDONALD OBSERVATORY, Science, 167, 368 (1970) (With C.O. Alley et al.)

THE LUNAR LASER RANGING EXPERIMENT, Proc. of the Conference on Experimental Tests of Gravitation Theories, Pasadena, 1970 (JPL Tech. Memo 33-499), with P. L. Bender et al.

LASER RANGING RETRO-REFLECTOR: CONTINUING MEASUREMENTS AND EXPECTED RESULTS, Science, 167, 468 (1970) (with C. O. Alley et al.)

LASER RANGING RETRO-REFLECTOR Apollo 14 Preliminary Science Report NASA SP-272, 1971, p. 215, (with J. E. Faller et al.)

A NEW INTERFEROMETRIC TECHNIQUE FOR VERY HIGH SPATIAL RESOLUTION, Bulletin Amer. Astron. Soc. 3, 244, 1971.

FAR-FIELD DIFFRACTION PATTERN FOR CORNER REFLECTORS WITH COMPLEX REFLECTION COEFFICIENTS, with R. F. Chang, C. O. Alley, and M. Pittman, J.O.S.A. 61, 431, April 1971.

LASER RANGING AT McDONALD OBSERVATORY: BIMONTHLY REPORTS, Feb.-April 1970 Tech. Report 70-106, April-June 1970 Tech. Report 71-006, June-August 1970 Tech. Report 71-031, August-December 1970 Tech. Report 71-083.

FUTURE POSSIBILITIES FOR LUNAR LASER RANGING EXPERIMENT (with C. O. Alley and S. K. Poultney) Space Research, Vol. XII Proceedings of the Fourteenth Plenary Session of COSPAR, Seattle 1971 (in press), Akademie-Verlag, Berlin 1972.

LUNAR RANGING AT McDONALD OBSERVATORY Space Research Vol. XII, Proceedings of the Fourteenth Plenary Session of COSPAR, Seattle 1971, p. 219-259, Akademie-Verlag, Berlin 1972, (with C. O. Alley and S. K. Poultney).

LUNAR RANGING AT McDONALD OBSERVATORY (with E. S. Silverberg and S. K. Poultney, Space Research, Vol. XII Proceedings of the Fourteenth Plenary Session of COSPAR, Seattle 1971 (in press), Akademie-Verlag, Berlin 1972.

OPTICAL SYSTEMS AND STATION PROCEDURES FOR THE SURVEYOR VII LASER POINTING TEST, Analysis of Surveyor Data, NASA TR #32-1443, (with M. S. Shumate, C. O. Alley, L. A. Allen et al.) 1969.

CURRENT STATUS AND FUTURE PROGRESS OF LUNAR LASER RANGING, Symposium #48 IAU @ Morioka, Japan.

LASER RANGING RETRO-REFLECTOR Apollo 15, Preliminary Science Report, NASA SP289, 1972, p. 14 (with J. E. Faller et al.).

A SELF-CONSISTENT SET OF SURFACE COORDINATES FOR THE APOLLO LUNAR LASER RETRO-REFLECTORS DEDUCED FROM LASER RANGE MEASURES (with J. D. Mulholland, H. H. Plotkin et al.) Space Research, Vol. XIII Proceedings of the Fifteenth Plenary Session of COSPAR, Seattle, 1972 (in press), Akademie-Verlag, Berlin 1972.

CANONICAL TRANSFORMATION AND QUADRATIC HAMILTONIANS, with E. Saletan, II Nuovo Cimento, 9B, 143, 1972.

LUNAR LASER RANGING WITH DECIMETER ACCURACY, Bull. Amer. Astrono. Soc. 4, 219, 1972.

SECOND GENERATION TIMING SYSTEM FOR APOLLO LUNAR LASER RANGING EXPERIMENT, D. G. Currie, C. A. Steggerda, J. D. Rayner, and A. Buennagel, Proceedings of the Fourth Annual NASA and Department of Defense Precise Time and Time Interval (PTTI) Planning Meeting, Goddard Space Flight Center, Greenbelt, Maryland, November 14-16, 1972.

OPTICAL PROPERTIES OF THE APOLLO LASER RANGING RETROREFLECTOR ARRAYS (with R. F. Chang, C. O. Alley, and J. E. Faller) Space Research, Vol. XIII Proceedings of the Fourteenth Plenary Session of COSPAR, Seattle 1971 (in press), Akademie-Verlag, Berlin 1972.

THE LUNAR LASER RANGING EXPERIMENT, Science 182, 229, (1973) (with P. L. Bender et al.)

FOUR STELLAR DIAMETER MEASUREMENTS BY A NEW TECHNIQUE: AMPLITUDE INTERFEROMETRY, D. G. Currie, S. L. Knapp, and K. M. Liewer, the Astrophysical Journal, 1 January 1974.

AMPLITUDE INTERFEROMETRY AND HIGH RESOLUTION IMAGE INFORMATION, Optical Propogation Through Turbulence, edited by (Topical Meeting of OSA) July 1974, University of Colorado Press.

LIBERATION AND LUNAR MOMENTS OF INERTIA CONSTRAINTS FROM LUNAR LASER RANGING, Trans. Amer. Geophysical Union, Vol. 55, p. 217, 1974.

ON A PHOTON COUNTING ARRAY USING THE FAIRCHILD CCD201, by Douglas G. Currie, presented at Symposium on Charged Coupled Device Technology for Scientific Imaging Applications at JPL, also University of Maryland Technical Report # 75-082, March 1975.

ON THE EFFECTIVE TEMPERATURE OF α HERCULIS A, D. G. Currie, S. L. Knapp, and K. M. Liewer, The Astrophysical Journal, Vol. 198, No. 3., Part 1, June 1975.

Publication Continued

AMPLITUDE INTERFEROMETRY AND DIFFRACTION LIMITED IMAGE PROCESSING, Optical Society of American Topical Meeting on Imaging in Astronomy, June 18-21, 1975.

FUTURE SYSTEMS, proceedings of the Second Workshop on Tracking Instrumentation held at the Technical University of Prague, Prague, 11-16 August 1975, edited by G. C. Weiffenbach and K. Hamal

THE PRELIMINARY SINGLE SCAN DATA RECORDING SYSTEM, University of Maryland Technical Report #76-038, September 1975.

A PRACTICAL STELLAR AMPLITUDE INTERFEROMETER, with K. M. Kiewer, D. G. Currie, and S. L. Knapp, presented at the Annual Meeting of the Optical Society of America, 23 October 1975.

ON AMPLITUDE INTERFEROMETRY FOR HIGH-ANGULAR-RESOLUTION ASTRONOMY, by Douglas G. Currie, presented at the Annual Meeting of the Optical Society of America, 23 October 1975.

AN INTENSIFIED CHARGE COUPLED DEVICE FOR EXTREMELY LOW LIGHT LEVEL OPERATION, 1975 International Conference on the Application of Charge Coupled Devices, sponsored by the Naval Electronics Laboratory, 29 October 1975.

EXTREMELY HIGH SPACIAL RESOLUTION - OPTICAL ASTRONOMY (USING AMPLITUDE INTERFEROMETRY) talk given at AMES Research Laboratory, 7 March 1976.

NEW TEST OF THE EQUIVALENCE PRINCIPLE FROM LUNAR LASER RANGING, with J. G. Williams, R. H. Dicke et al. Phys. Rev. Lett. Vol. 36, No. 11, 15 March 1976.

PRECISE SATELLITE RANGING USING THE "SHINY BALL" SATELLITE, with C. O. Alley, S. K. Poultney, F. Hoge, and J. T. McGoogan, to be submitted.

STELLAR DIAMETER MEASUREMENTS BY AMPLITUDE INTERFEROMETRY 1972 - 1976, R. Braunstein, S. Knapp, D. G. Currie and k. Liewer, University of Maryland Technical Report #76-125, March 1976.

PHOTON COUNTING ARRAY PHOTOMETER, with J. C. Choisser, SPIE/SPSE Technical Symposium East, 23 March 1976.

ON THE USE OF THE OPTICAL VERY LONG BASELINE INTERFEROMETER, Conference on Extra Solar Planetary Detection Workshop, at the University of California Santa Cruz Campus, 24 and 25 March 1976.

OPTICAL INTERFEROMETRY, presented at the Conference on Radio Interferometry and Astrometry for Universal Time, 8 April 1976.

AMPLITUDE INTERFEROMETRY PROGRAM FOR EXTREMELY HIGH RESOLUTION IMAGING, June 1976.

COMMENTS ON A DUST DETECTOR FOR USE ON THE SURFACE PENETRATOR MISSION, August 1976.

ON A PHOTON COUNTING ARRAY PHOTOMETER, IAU Colloquim #40, Meudon, France, 7 September 1976., also University of Maryland Technical Report 77-037.

EARTH-ROTATION MEASURED BY LUNAR LASER RANGING", _Science_ Vol. 173, 997-999, 10 September 1976, A. Stolz, Bender, _et al_.